

Magnetic field and ion-optical simulations for the optimization of the Super-FRS

E. Kazantseva

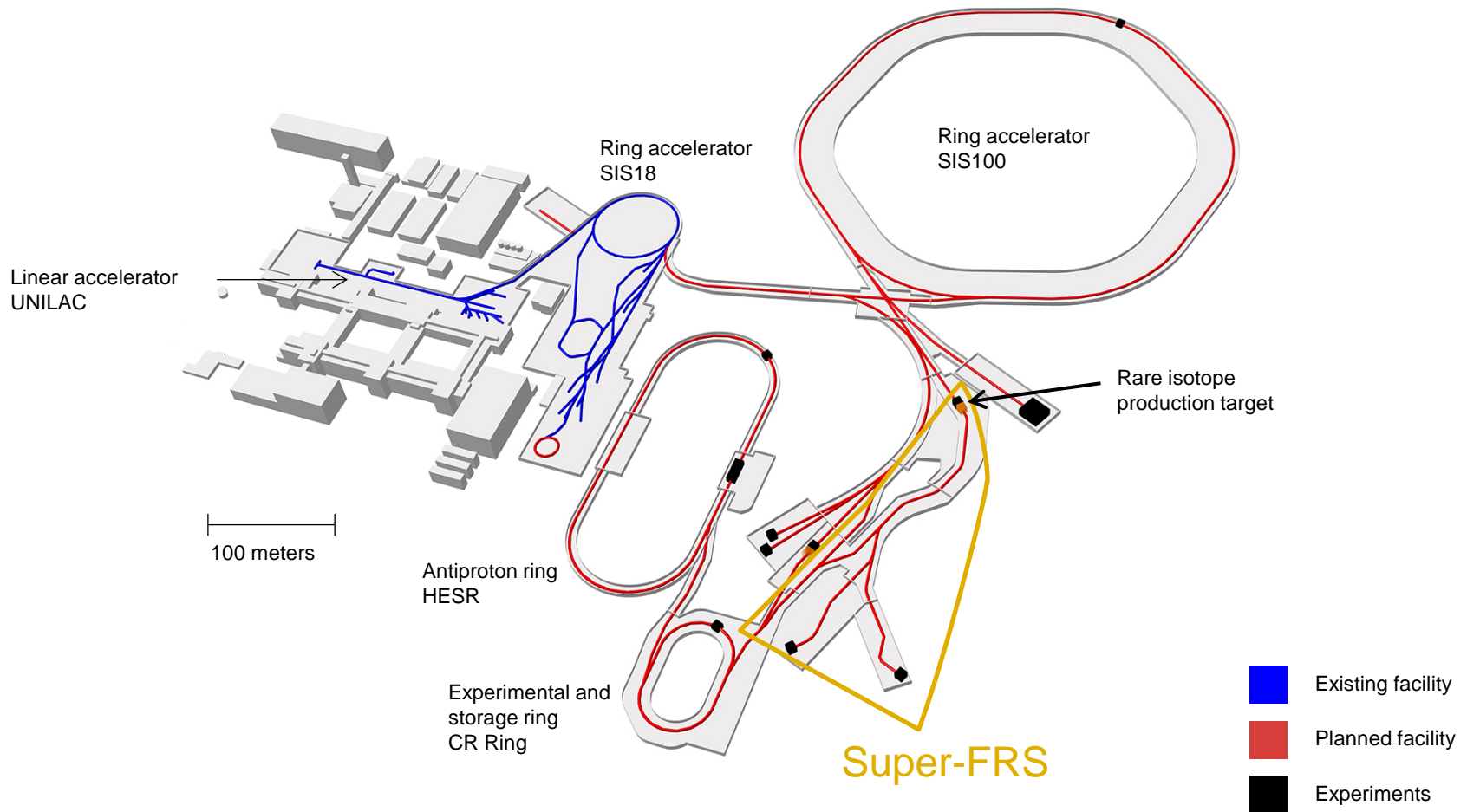


TECHNISCHE
UNIVERSITÄT
DARMSTADT



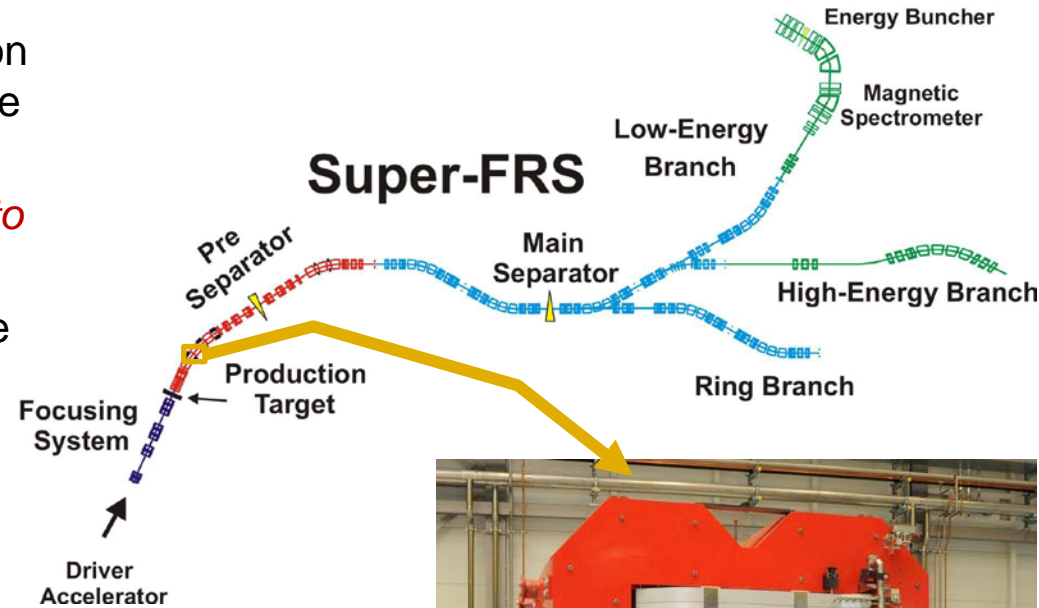
- **Introduction**
- **Computing high-order realistic Taylor transfer maps:**
 - Measurements/simulations the B -field
 - Setting the reference trajectory in dipoles
 - Obtaining B -field as smooth functions of X, Y, Z, l
 - Integration of equations of motion of the reference particle in the differential algebraic (DA) framework.
- **Super-FRS optics application:**
 - Fitting the multipole strengths
 - Comparison of different approaches
 - Separator/Spectrometer mode for different magnetic rigidities
- **Summary, outlook**

Super-FRS project at GSI FAIR



Motivation

- For high transmission rates and resolution of Super-FRS large aperture magnets are required
 - *Long fringe fields, inhomogeneities due to mechanical tolerances*
- High experimental flexibility leads to wide range of the magnetic field values
 - *Non-linear magnetization and saturation effects*
- The magnetic fields have to be changed many times a day during experiments
- Many magnets with long magnetization cycles are involved (2 min from 0 to B_{\max})
 - *Manual tuning is too time consuming*
- *Accurate and fast model considering realistic magnetic fields from measurements or accurate 3D simulations is required for efficient operation of Super-FRS*



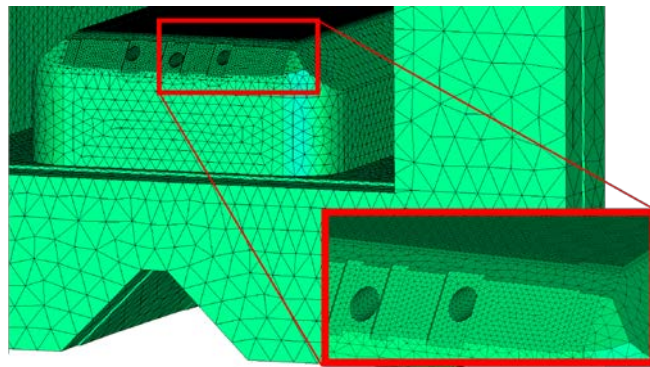
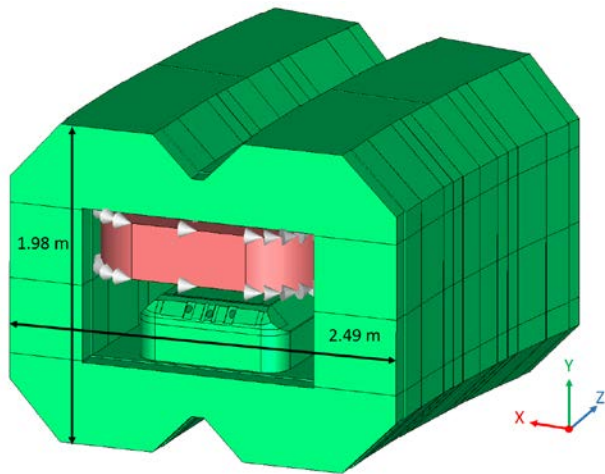
Prototype of the 11° radiation resistant NC dipole

Steps to extract accurate high order Taylor transfer maps

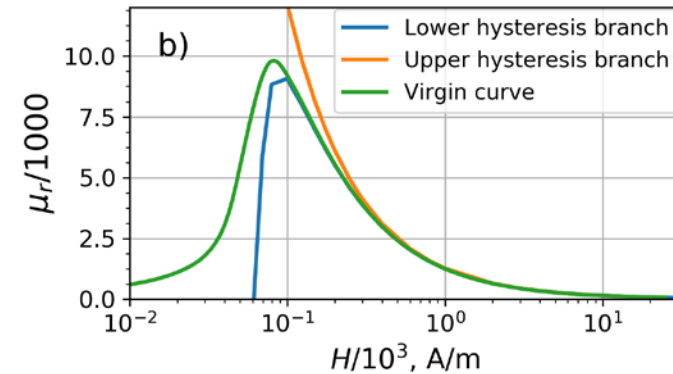
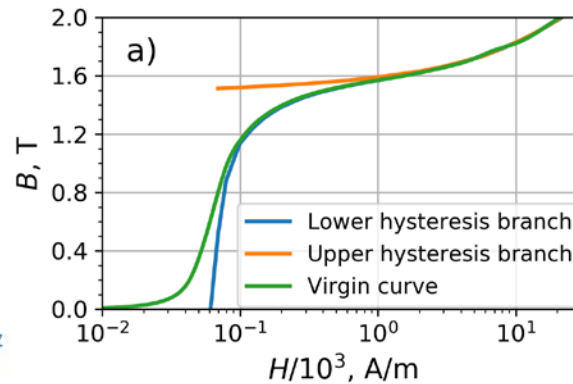


1. Measure/simulate the B-field
2. Set the reference trajectory (dipoles)
3. Obtain B -field as smooth functions of X, Y, Z, I
4. Integrate equations of motion in DA framework.

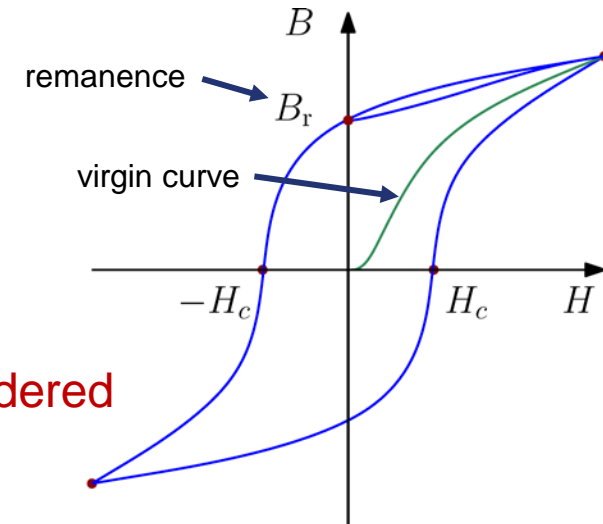
FEM simulations with CST EMS



Measured magnetization curves

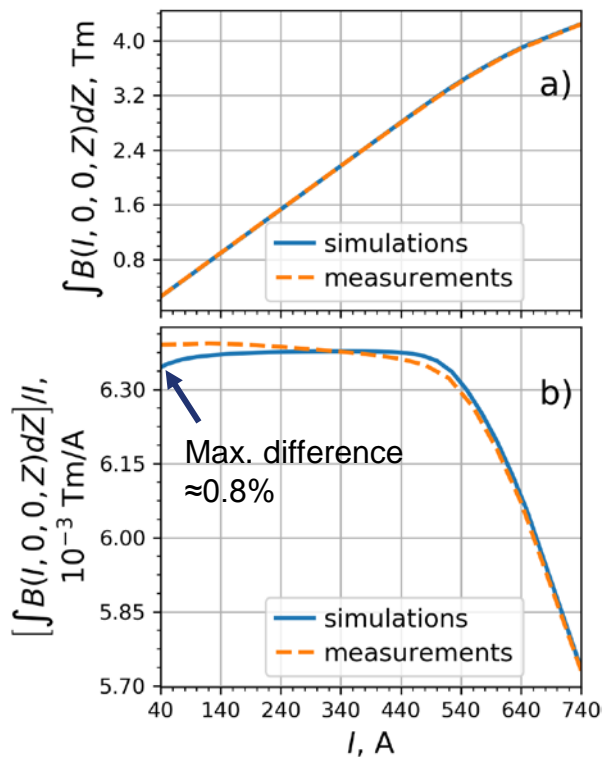


- Accurate geometry
- Measured virgin curve
- Unipolar current source
- There is remanent field
- Remanence is not considered

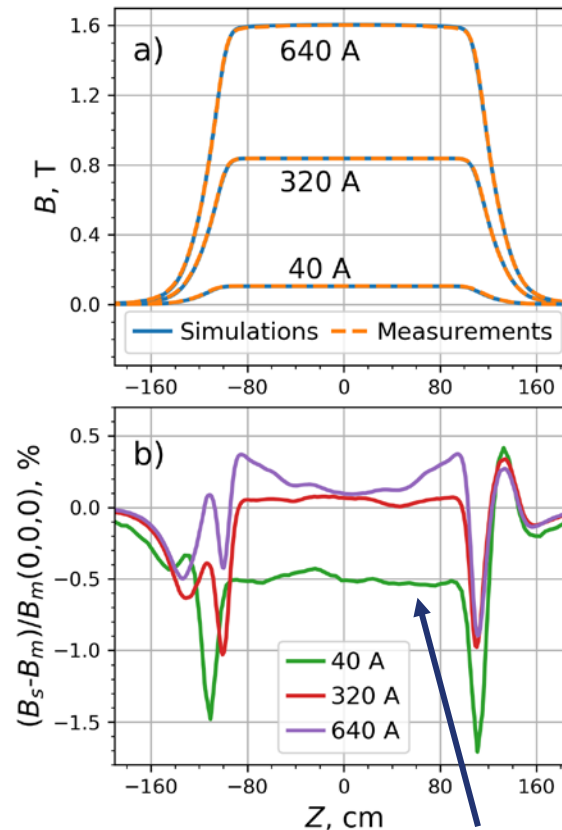


Benchmarking of simulations with the measurements

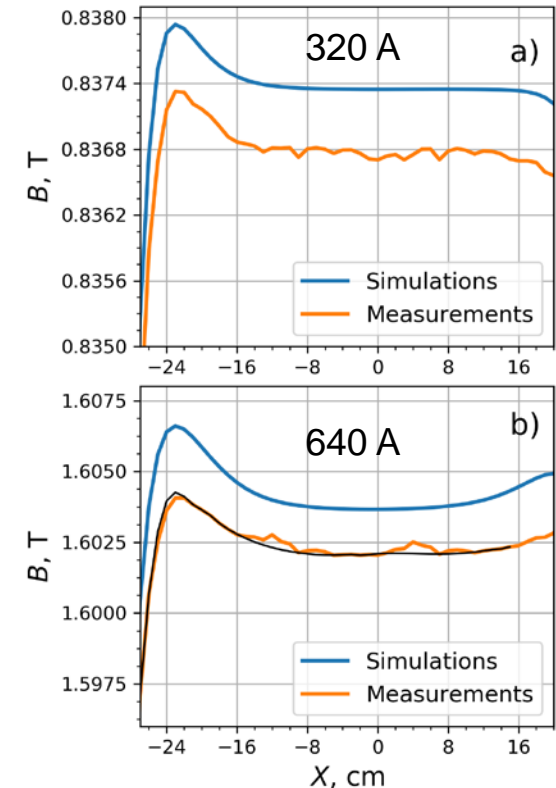
Excitation curve



B_Y along Z axis



B_Y along X axis



“Missing” remanence in FEM model

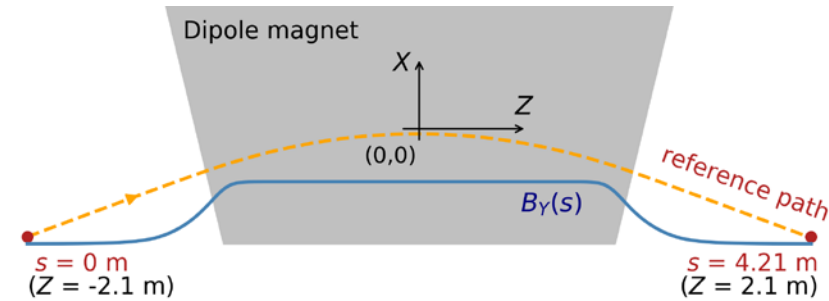
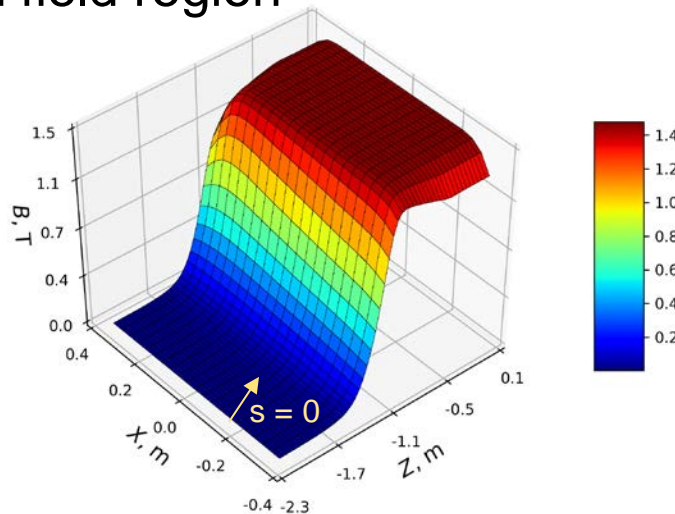
Criteria to set a reference trajectory in a dipole

- Deflecting angle in the dipole must be **fixed** for all rigidities from **2 to 20 Tm**

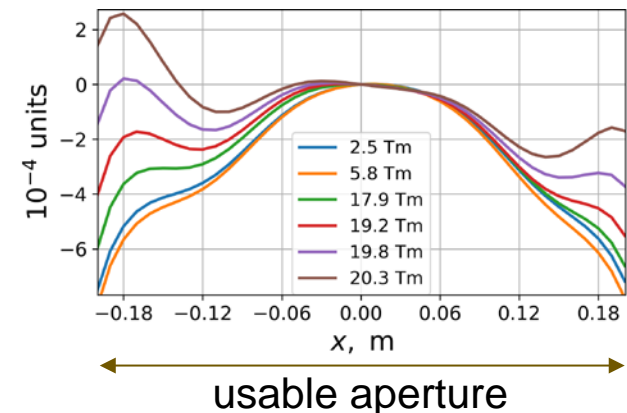
$$\theta = \int_S \frac{B_y(I)}{B\rho} ds$$

- Reference trajectory must be centered in a good field region

B in Y=0
for I = 575 A



Integral field non-uniformity for different rigidities

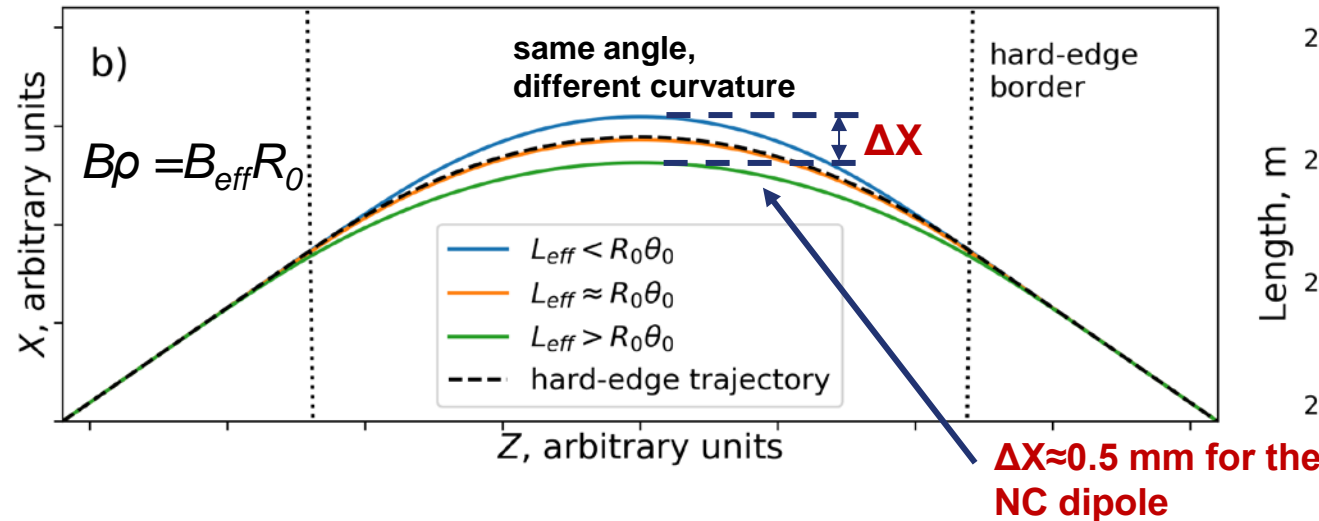
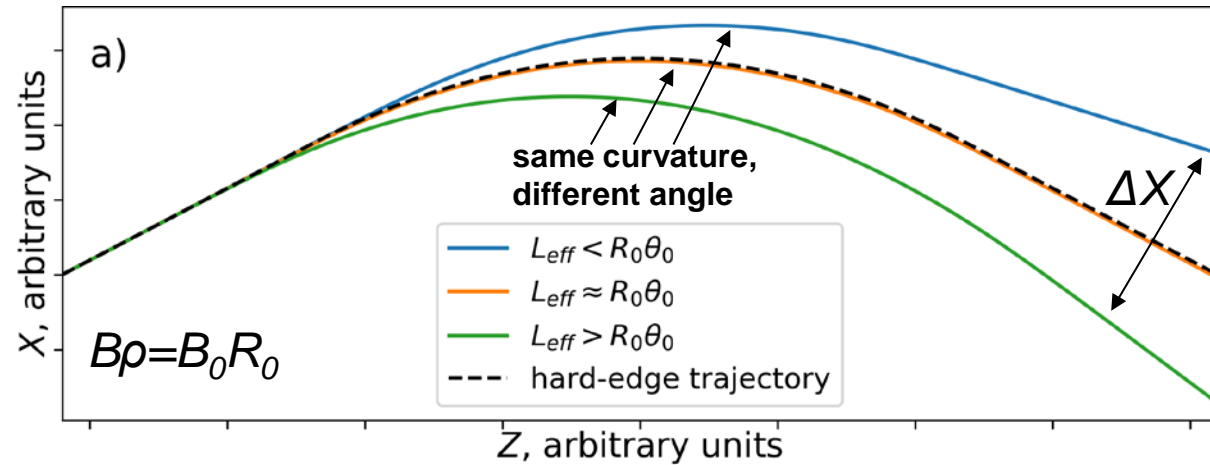


Fixing R_0 versus fixing θ_0

- Effective length $L_{\text{eff}}(I) := \frac{1}{B_0(I)} \int_S B_y(I) ds$ is equal $R_0\theta$ if $B\rho = B_0R_0$
- θ drops with L_{eff}
- If $B\rho \neq B_0R_0$ then L_{eff} is not informative
- It is possible to fix θ_0 by varying $B\rho(l)$ or l
- Using $B_{\text{eff}} = B\rho/R_0$ one gets $L_{\text{eq}}(I) := \frac{1}{B_{\text{eff}}(I)} \int_S B_y(I) ds = R_0\theta(I)$
- In optimal case $L_{\text{eq}} = R_0\theta_0$

Actual
deflecting
angle

Fixing R_0 versus fixing θ_0



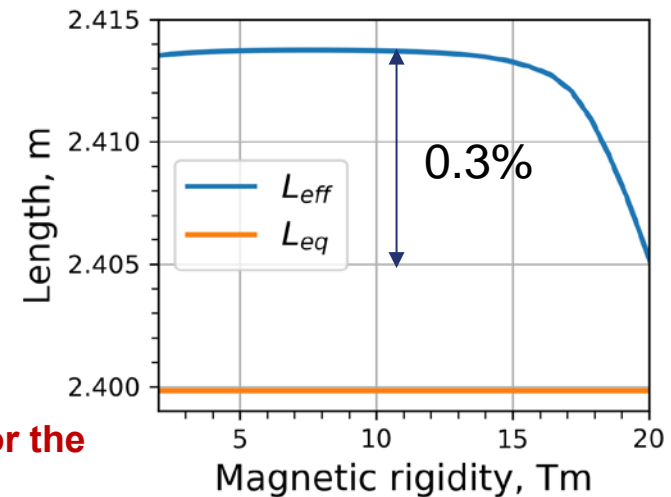
NC SFRS dipole:

$\Delta\theta(2-20 \text{ Tm}) = 1 \text{ mrad}$ ($0.56\%\theta_0$)
 $\Delta X = 1.2 \text{ cm}$ after stage of 3 dipoles.

SC (9.75°) dipole:

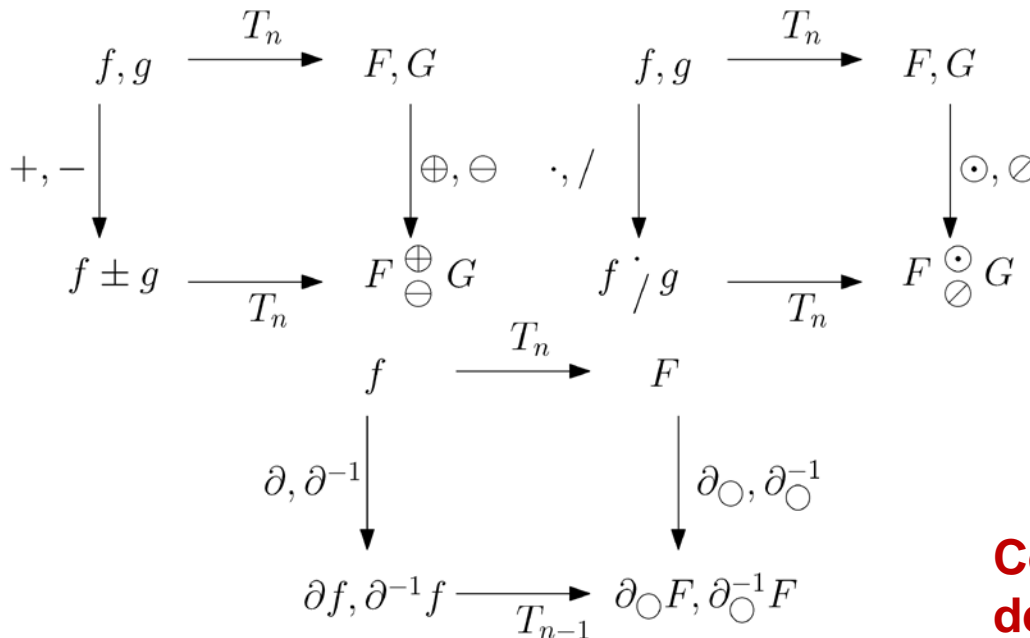
$\Delta\theta(2-20 \text{ Tm}) = 1.9 \text{ mrad}$ ($1.1\%\theta_0$)

L_{eff} and L_{eq} for NC SFRS dipole.
 $L_{eq}(l)$ was adjusted for each $B\rho$ to result in $\theta_0 R_0$



The Differential Algebra $_nD_v$

Differential Algebraic (DA) vector: Ordered vector with all Taylor coefficients of an expansion in point \mathbf{x} of a real analytic (r.a.) function f in v variables up to order n .



T_n – extraction of Taylor coefficients up to order n

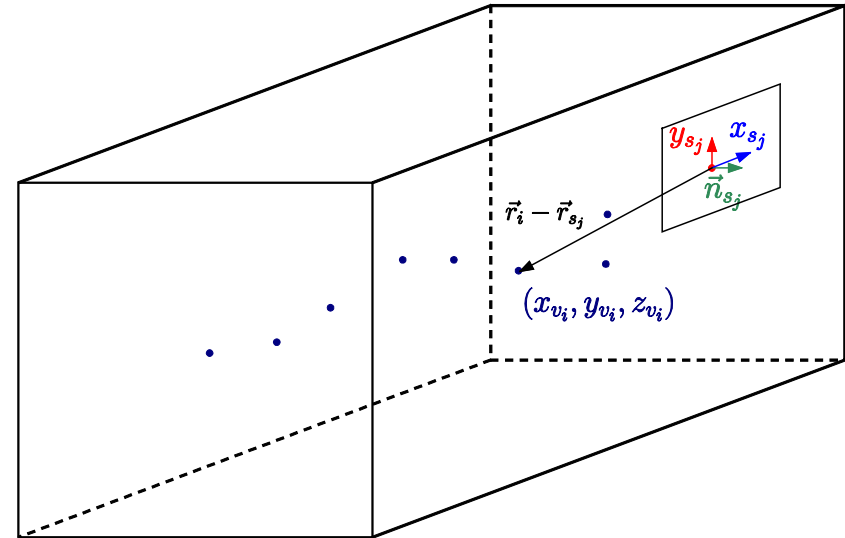
DA is a TPSA with defined operations of derivation ∂ and antiderivation ∂^{-1}

Complex problems with integrals and derivatives of r.a. functions can be solved in DA framework using mere arithmetics operations

Commuting diagram of the DA structure

Surface Integration Helmholtz Method (SIHM)

$$\begin{aligned}\vec{B}(\vec{r}) &= \vec{\nabla} \cdot \varphi(\vec{r}) + \vec{\nabla} \times \vec{A}(\vec{r}) \\ \varphi(\vec{r}) &= \frac{1}{4\pi} \int_{\partial\Omega} \frac{\vec{n}(\vec{r}_s) \cdot \vec{B}(\vec{r}_s)}{|\vec{r} - \vec{r}_s|} ds, \\ \vec{A}(\vec{r}) &= -\frac{1}{4\pi} \int_{\partial\Omega} \frac{\vec{n}(\vec{r}_s) \times \vec{B}(\vec{r}_s)}{|\vec{r} - \vec{r}_s|} ds.\end{aligned}$$



Integration on each surface element using DA ∂^{-1} operation

Integrands expanded in surface and volume coordinates

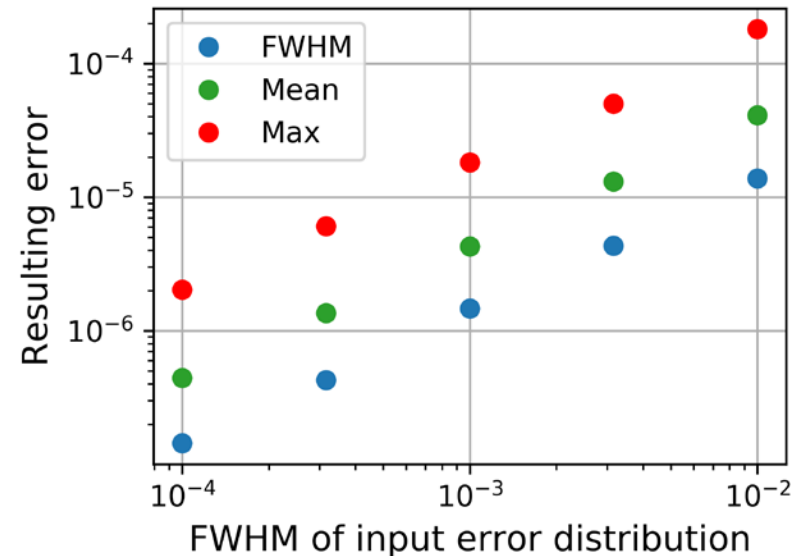
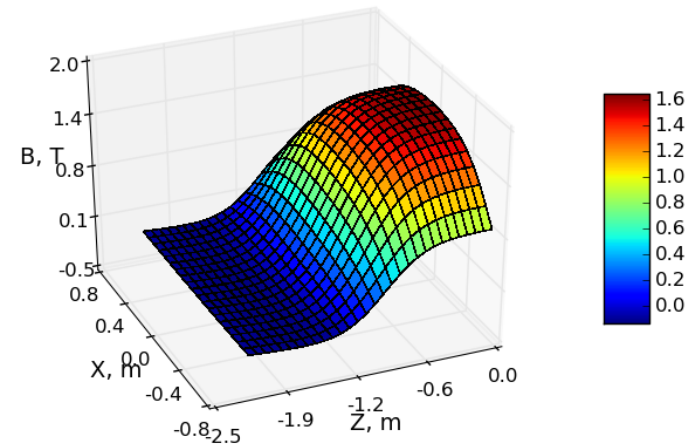
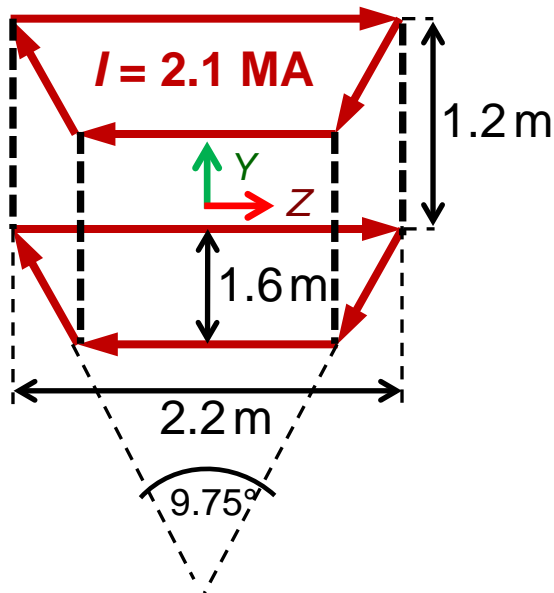
Resulting B is harmonic

S. Manikonda, High Order Finite Element Methods to Compute Taylor Transfer Maps, PhD Dissertation, 2006;
M. Berz, Modern Map Methods in Particle Beam Physics, 1999

Robustness of SIHM: analytic example

- Biot-Savart magnetic field from a current wire configuration.

$$\mathbf{B}(\mathbf{r}) = \frac{\mu_0}{4\pi} \int_C \frac{I d\mathbf{l} \times \mathbf{r}'}{|\mathbf{r}'|^3}$$



Obtaining accurate $B(X, Y, Z, I)$ polynomials

- Using superposition principle and least squares fit, $B_{X,Y,Z}(I)$ can be decomposed in

$$B_{\alpha}(I) \approx b_0^{\alpha} + b_1^{\alpha}(I - I_0) + b_2^{\alpha}(I - I_0)^2 + \dots + b_n^{\alpha}(I - I_0)^n$$

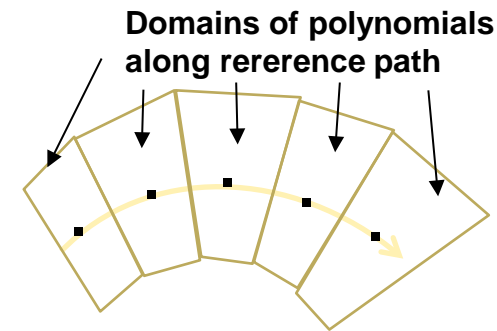
where $\alpha \in \{X, Y, Z\}$

- DA SIHM can be applied to b_i^{α} .

- Radius of convergence of resulting DA vectors \leq pole gap

- Solution approach:

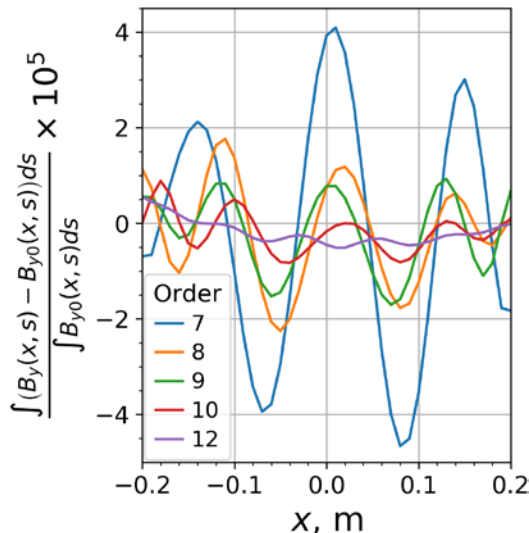
- SIHM calculation of low (2nd) order polynomials of $b_i^{\alpha}(X, Z)$ in 2D array of points
- least squares fit of higher orders polynomials in midplane.
- DA fixed point theorem reconstruction of harmonic off-plane field.



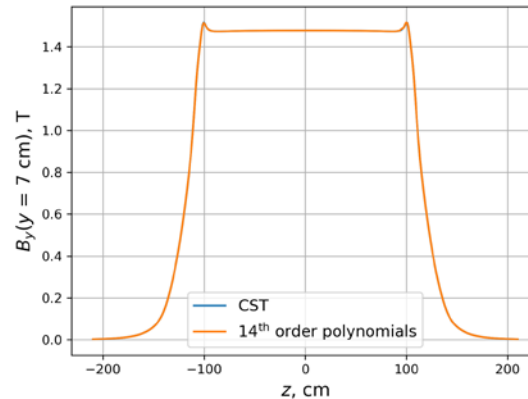
Accuracy of the resulting polynomials

- Polynomials compared to FEM output
- Many polynomials used in s direction, each time only one in x direction.

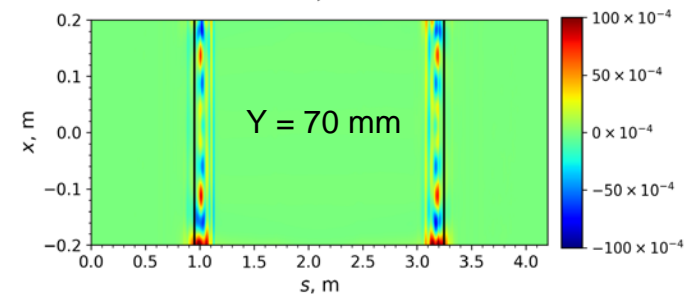
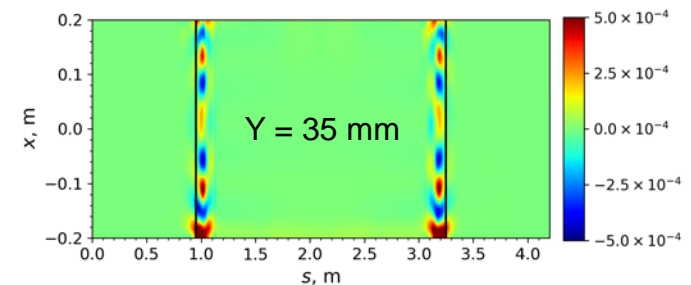
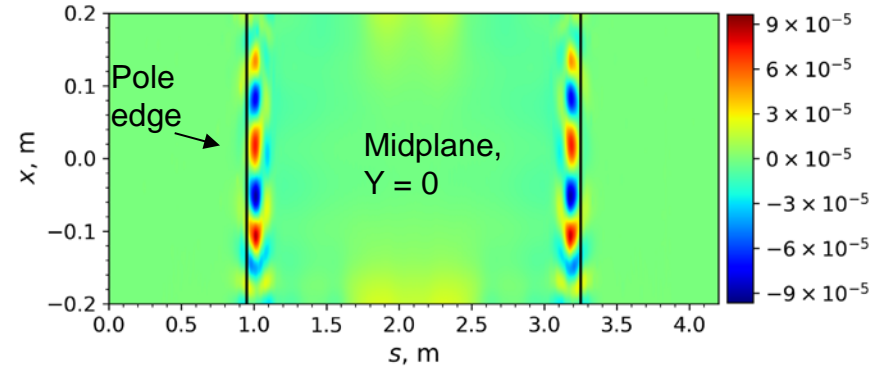
Integrated relative error for I = 575 A in Y = 0 plane



Field values for I = 575 A in Y = 70 mm plane



Relative error for I = 575 A and 10th order polynomials



Within the method the off-plane errors can be reduced only by using higher orders.

Beam physics ODEs

- $\vec{z}(s) = \vec{f}(s, \vec{z}(s_0)) = (x, a, y, b, l, \delta_K)|_s$
- ODEs for flat reference trajectory and conserved energy:

$$x' = a(1 + hx) \frac{p_0}{p_s},$$

$$y' = b(1 + hx) \frac{p_0}{p_s},$$

$$l' = \left((1 + hx) \frac{1 + \eta \frac{p_0}{p_s}}{1 + \eta_0 \frac{p_0}{p_s}} - 1 \right) \frac{\eta_0 + 1}{\eta_0 + 2},$$

$$a' = \left(b \frac{B_s}{B\rho_0} \frac{p_0}{p_s} - \frac{B_y}{B\rho_0} \right) (1 + hx) + h \frac{p_0}{p_s},$$

$$b' = \left(\frac{B_x}{B\rho_0} - a \frac{B_s}{B\rho_0} \frac{p_0}{p_s} \right),$$

$$\delta' = 0$$

$h = B\rho/B_y(x, s)$ – curvature, $\eta = K/E_0 = \gamma - 1$

$B\rho$ can be added as an extra parameter into the variables, dependent on it: η , h , p_0 , p_s , $B_{x,y,s}$ to obtain $B\rho$ -dependent transfer maps

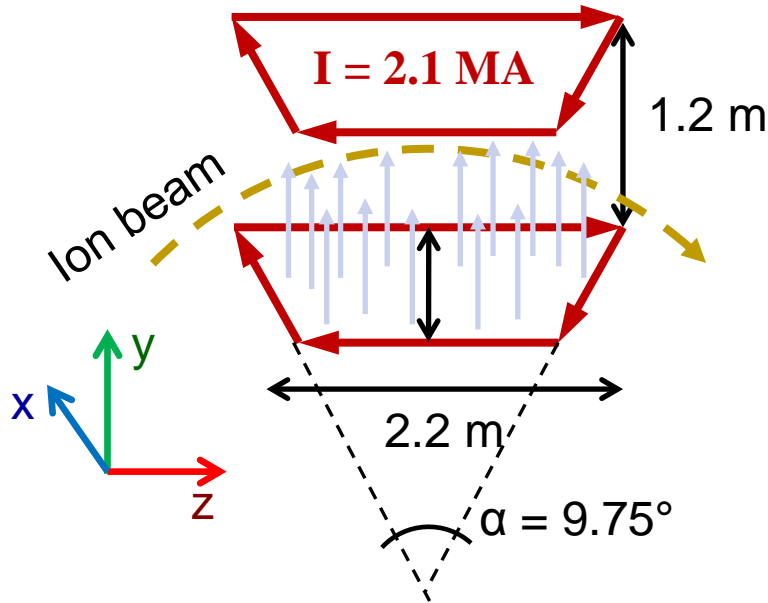
DA Transfer Maps



x	a	y	b	Order	Exponents			
$\partial x_f / \partial x_i$	$\partial a_f / \partial x_i$	$\partial y_f / \partial x_i$	$\partial b_f / \partial x_i$	1	1	0	0	0
$\partial x_f / \partial a_i$	$\partial a_f / \partial a_i$	$\partial y_f / \partial a_i$	$\partial b_f / \partial a_i$	1	0	1	0	0
...								
$2\partial^2 x_f / \partial x_i^2$	$2\partial^2 a_f / \partial x_i^2$	$2\partial^2 y_f / \partial x_i^2$	$2\partial^2 b_f / \partial x_i^2$	2	2	0	0	0
...								
$j!k!!!m! \partial^{j+k+l+m} x_f / \partial x_i^j \partial a_i^k \partial y_i^l \partial b_i^m$	$j!k!!!m! \partial^{j+k+l+m} a_f / \partial x_i^j \partial a_i^k \partial y_i^l \partial b_i^m$	$j!k!!!m! \partial^{j+k+l+m} y_f / \partial x_i^j \partial a_i^k \partial y_i^l \partial b_i^m$	$j!k!!!m! \partial^{j+k+l+m} b_f / \partial x_i^j \partial a_i^k \partial y_i^l \partial b_i^m$	$j+k+l+m$	j	k	l	m

Table 1 Example of the Taylor Transfer Map Structure for 4 variables: x, a, y, b

Accuracy of the resulting transfer maps



Initial phase volume:

$$x_i \in [-0.183 \text{ m}, 0.183 \text{ m}],$$

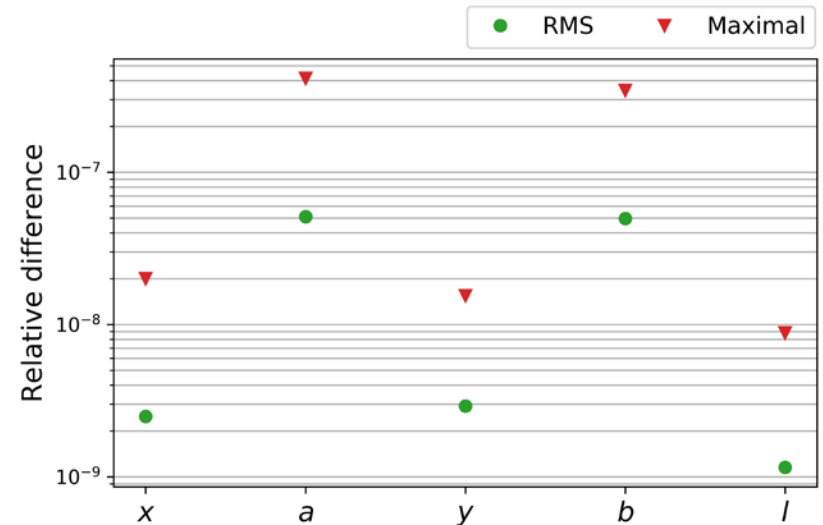
$$a_i \in [-0.219 \text{ mrad}, 0.219 \text{ mrad}],$$

$$y_i \in [-0.078 \text{ m}, 0.078 \text{ m}],$$

$$b_i \in [-0.513 \text{ mrad}, 0.513 \text{ mrad}],$$

$$\delta_i \in [-2.5\%, 2.5\%].$$

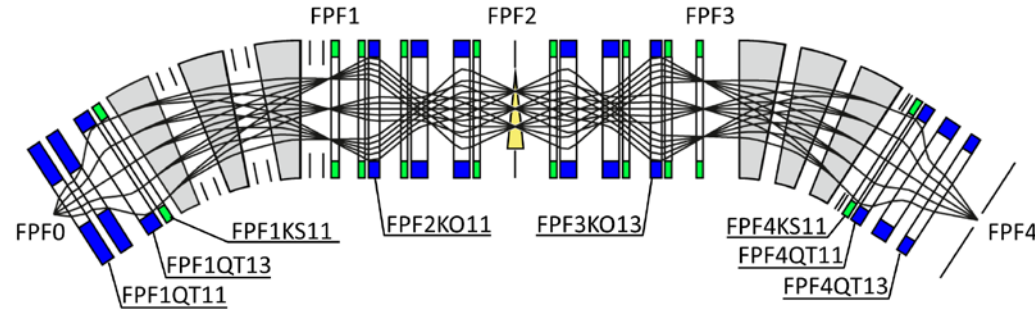
Similar as in
SFRS dipoles



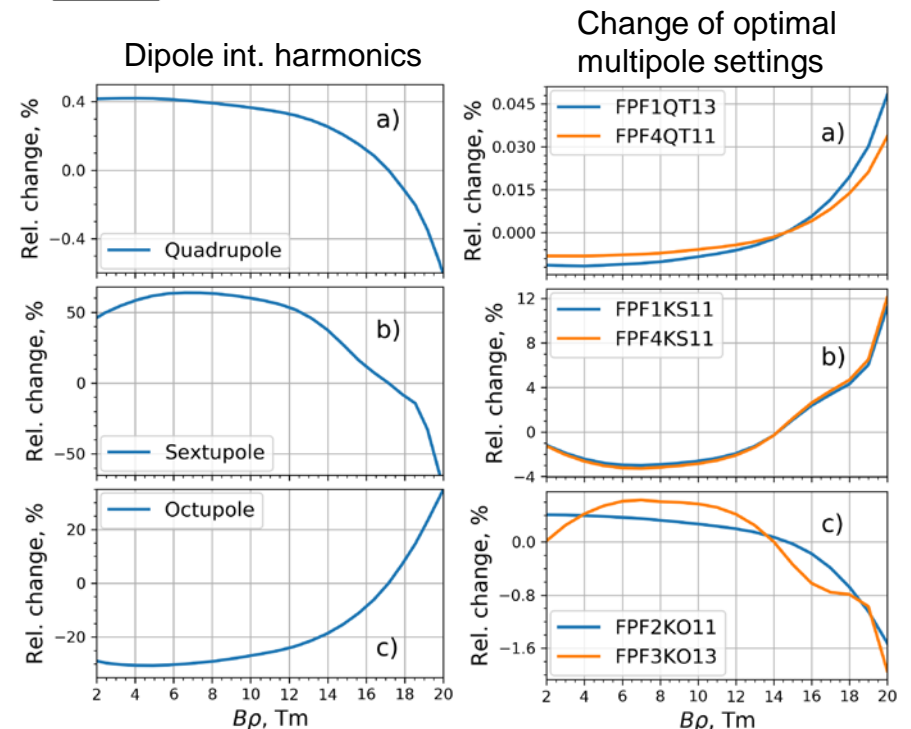
The error due to the numerical implementation of the method is much lower than the inevitable magnetic field instability!

Super-FRS preseparator optics with realistic dipole transfer maps

- One $B\rho$ - ΔE - $B\rho$ stage
- 3 NC and 3 SC dipoles
- Standard COSY transfer maps were used for multipoles
- Optics is optimized for design $B\rho$ range

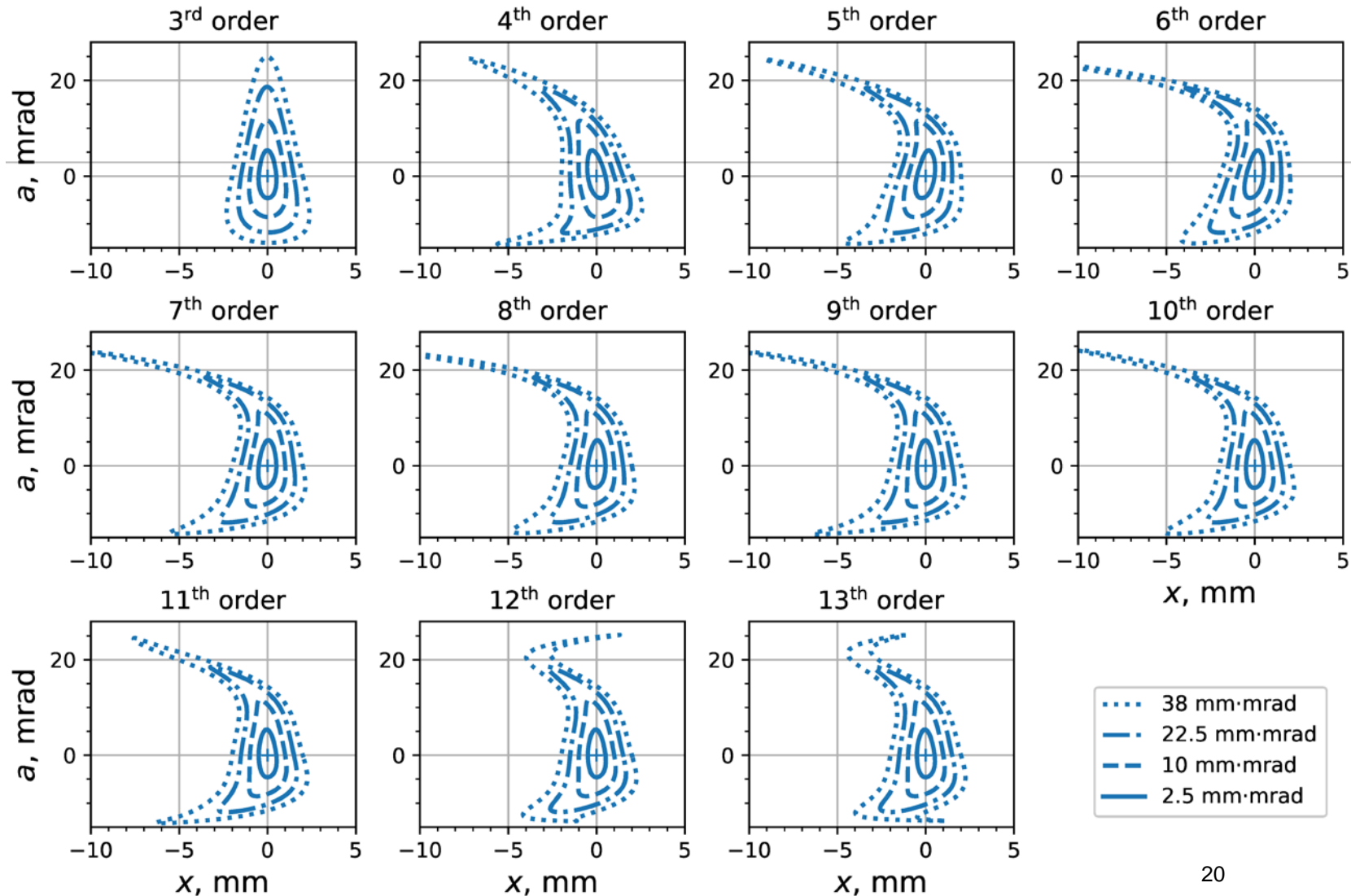


In optimal case the multipoles “compensate” the dipole inhomogeneity



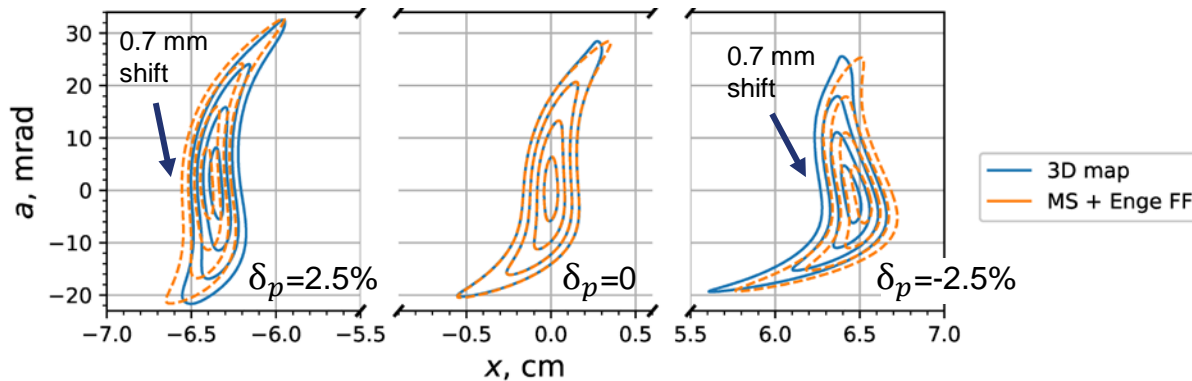
More details in E. Kazantseva et al., accepted in Nucl. Instr. Meth. A.

Maps of different orders: xa at FPF4



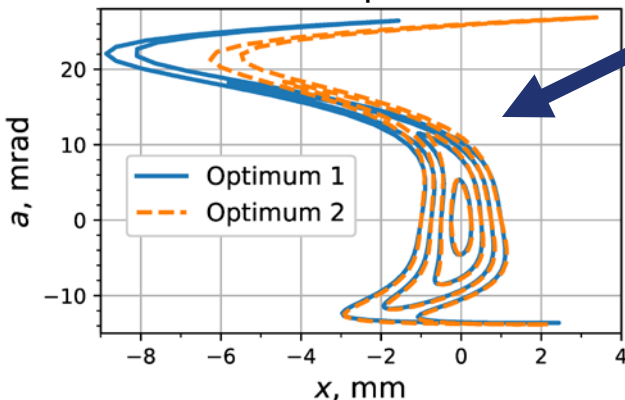
Comparison of 3D transfer maps with thick multipole maps MS + Enge FF

Dispersive plane FPF2



- **MS+Enge FF** maps are nearly as good as **3D** maps for dipoles
- Optimal settings are slightly different.

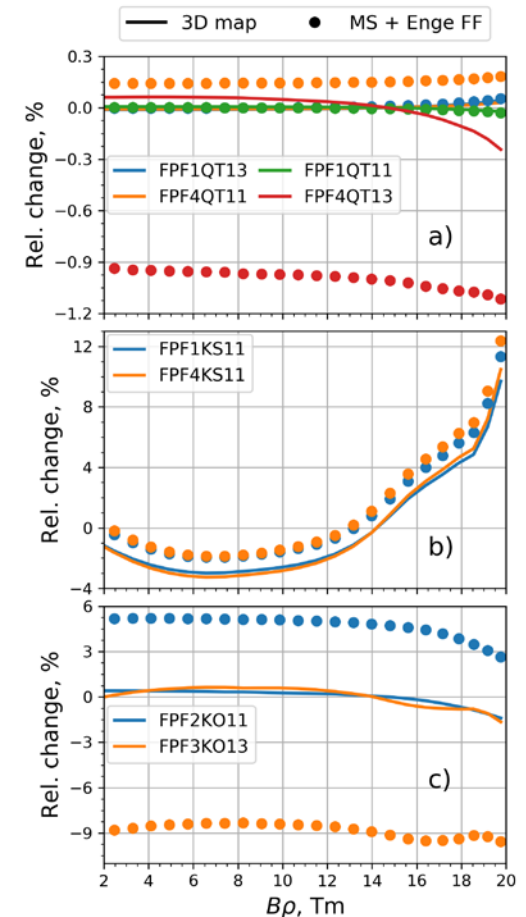
Achromatic plane FPF4



Optimum 1: **3D** maps + **3D** fit results
Optimum 2: **3D** maps + **MS+Enge** fit results

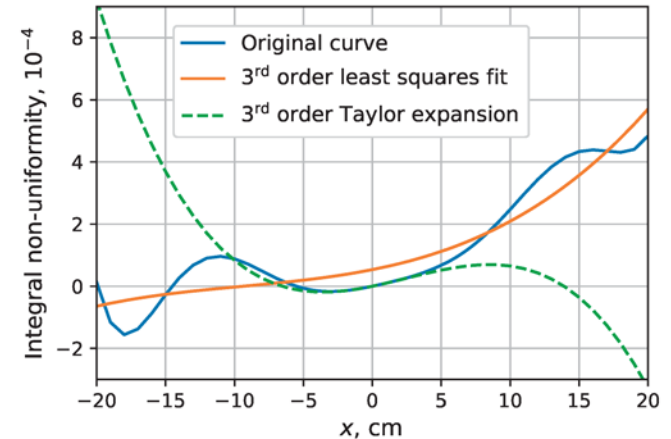
➤ The optimum with **MS+Enge** fit results seems to be even better.

Change of optimal multipole settings

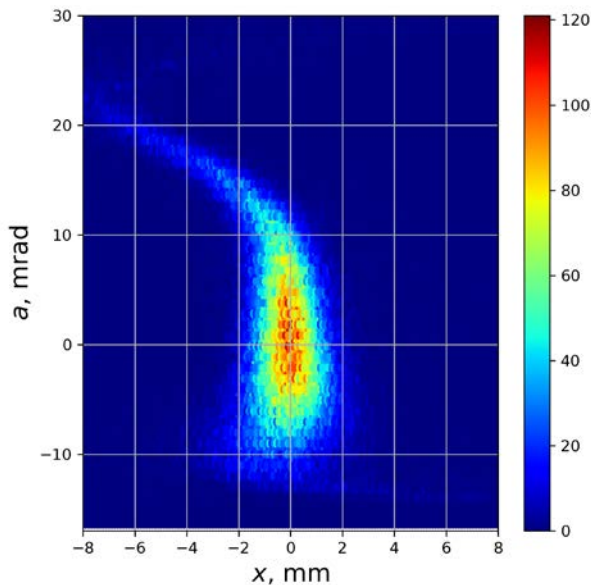


Correction by tuning available multipoles

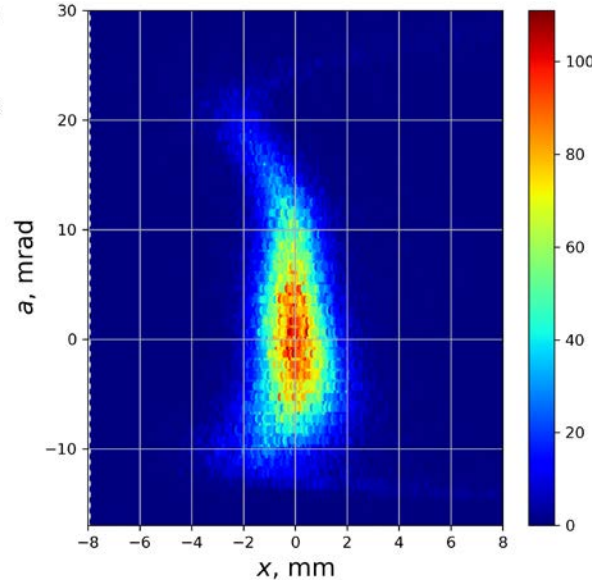
- **Maximum correction order = 3**
 - 3rd order transfer maps with least squares fitted integral multipoles can be used for fitting optics
 - Obtained optimal settings can be used in higher order calculations



13th order, optimal fit



13 order, coefficients
from 3rd order fit



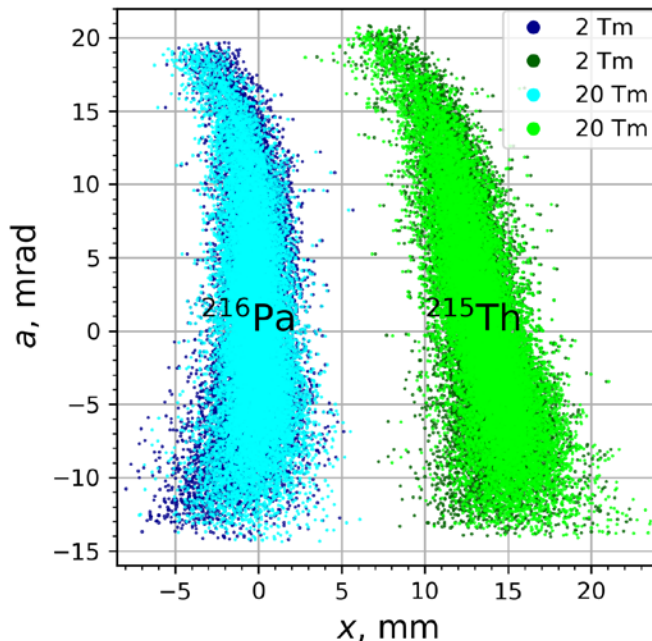
Horizontal phase space at FPF4 for initial Gaussian distribution with FWHM equal to design acceptance

$B\rho$ – dependent effects on the resolution: separator/spectrometer modes

Separator mode

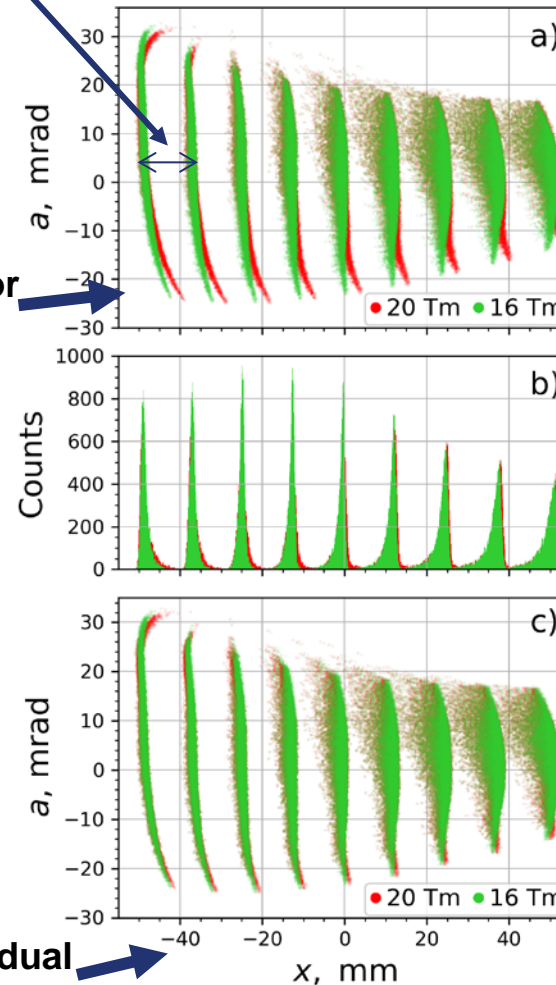
- Example: separation of ^{216}Pa from ^{215}Th
 - ^{216}Pa slowed down 14 Tm with Cu wedge
 - B distributions for 2 and 20 Tm
 - Degrader simulation with Lindhard-Sørensen theory

FPF4



$\Delta p/p = 1.2 \times 10^{-3}$ Spectrometer mode

Optimum for
16 Tm in all
cases



- Dispersion of stages added
- 1st stage of Super-FRS repeated 4 times to imitate the effect of the whole Super-FRS
- Monoenergetic slices with identical transversal phase space distributions

Summary

- An algorithm to obtain functional dependence of $B(X, Y, Z, I)$ with maintaining its harmonic property was developed by combining SIHM and least squares methods.
- An approach to generate accurate high-order rigidity-dependent transfer maps from 3D magnetic field was developed in *COSY INFINITY* and *Python 2.7* and applied to NC Super-FRS dipole.
- The introduction of L_{eq} allowed to minimize the saturation effects.
- NC dipoles do not contribute much in rigidity-dependent aberrations.
- Approach was suggested for compensation of high-order aberrations using low-order least squares fit of integral field non-uniformities.

Outlook:

- Taking the remanence into account using free open source tools (GetDP or FEniCS).
- Testing the approach with measured magnetic field (in collaboration with CERN)
- Application of the methods to all Super-FRS magnets
- Studying fringe field overlapping effects

Acknowledgements



TECHNISCHE
UNIVERSITÄT
DARMSTADT

- Dr. Helmut Weick
- Prof. Dr. Martin Berz
- Prof. Dr. Kyoko Makino
- Dr. Ravi Jagasia
- Dr. John Winfield
- Dr. Franz Klos
- Dr. Hanno Leibrock
- Dr. Peter Rottländer
- Dr. Carsten Mühle
- Dr. Eun Jung Cho

**Thank you
for the attention!**